A General <u>D</u>amage <u>I</u>nitiation and <u>E</u>volution <u>M</u>odel (DIEM) in LS-DYNA

<u>Thomas Borrvall</u>, Thomas Johansson and Mikael Schill, DYNAmore Nordic AB

Johan Jergéus, Volvo Car Corporation

Kjell Mattiasson, Volvo Car Corporation and Chalmers University of Technology

Paul DuBois, Consulting Engineer

1   Introduction

As the automotive industry is reducing the number of physical prototypes in favour of computer simulations during their design processes, a lot of demands is put on the accuracy of the virtual finite element models used for this purpose. In this context the mathematical modelling of fracture is of major importance and has been a field of intense research over the past 50 some years. There are numerous fracture models implemented in LS-DYNA, but as of tradition a fracture model is statically linked to the underlying constitutive model which in practice limits its usage to a single stage of the design process. Recently GISSMO [1,2,3] was introduced in an attempt to remedy this shortcoming by allowing the fracture model to be separated from the constitutive model, thus facilitating results from manufacturing simulations to be transferred to subsequent crash simulations. Behind GISSMO, the Damage Initiation and Evolution Model (DIEM) was developed in the same spirit and with similar capabilities, but this model has to the authors' knowledge not been used extensively. The intention with this paper is to present this latter fracture model and compare it with GISSMO and, to some extent, with CrachFEM [4] to which it has superficial similarities.
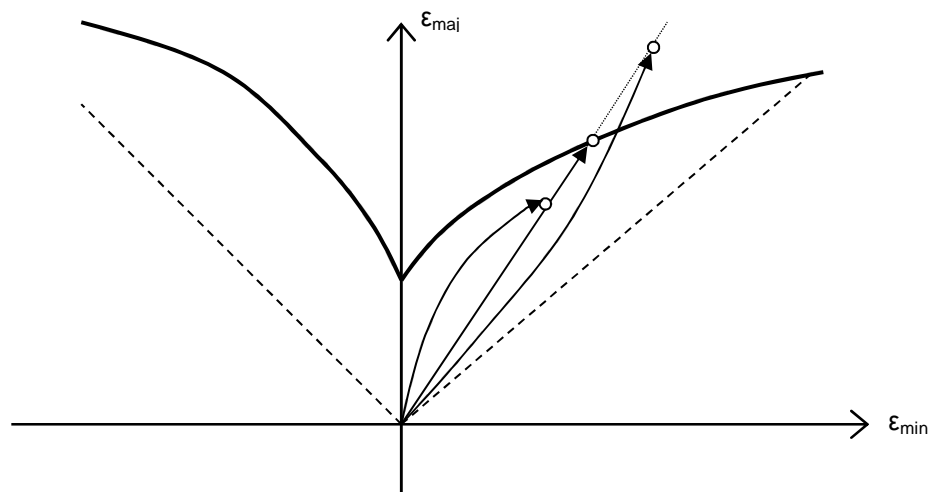
Fig 1 Illustration of an FLD diagram and fracture along linear and nonlinear strain paths.

2   Fracture modelling

2.1   Plastic instability and the FLD diagram

Failure in sheet metals are either due to material instability with localized deformation or fracture from initiation, growth and coalescence of voids, or a combination of the two. The onset of material instabilities depends to a great extent on the material properties including yield strength, strain hardening and rate dependency as well as geometry imperfections of the sheet. Usually plastic

instability with localized necking takes place before any other failure mechanism, and can either be mathematically predicted using for instance the Marciniak-Kuczynski method [5] or established through material tests. In either case, a common representation of the instability characteristics of a metal sheet is through a Forming Limit Curve (FLC) in a Forming Limit Diagram (FLD), as illustrated in Fig 1. The FLC is a function of the minor in-plane principal (plastic) strain

$$\varepsilon_{maj}^* = \varepsilon_{maj}^*(\varepsilon_{min})$$

and gives the points where instability occurs in the in-plane principal strain space. The safe zone is given by the inequality

$$\varepsilon_{maj} < \varepsilon_{maj}^*,$$

i.e., the area below the FLC curve, and the strains should typically reside in this region. The FLC curve is usually restricted to linear strain paths, i.e., straight lines in the FLD diagram, and for nonlinear paths instability may occur either below or above the FLC curve as illustrated in Fig 1.
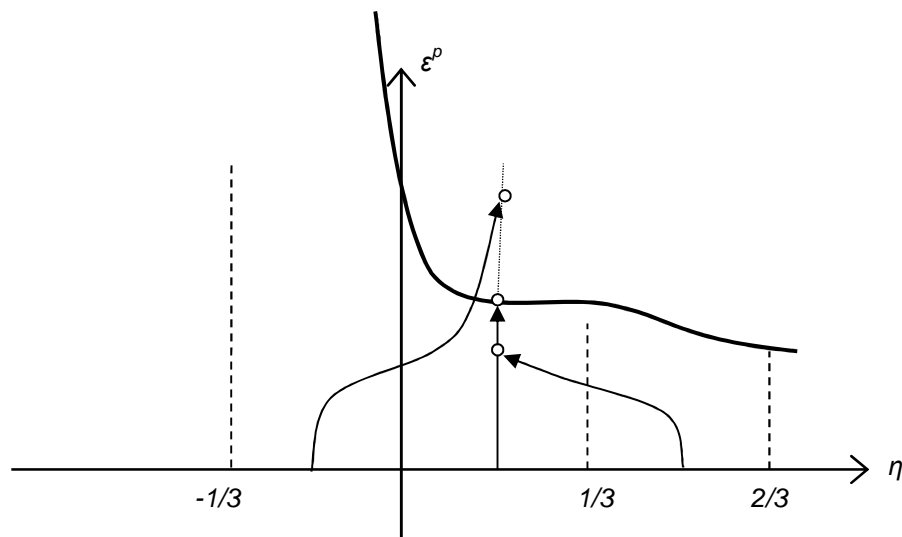
Fig 2 FLC curve represented as critical plastic strain versus triaxiality.

With the restriction to linear strain paths and von Mises associative plasticity, the FLC can be equivalently represented in terms of critical effective plastic strain as function of either triaxiality defined as the ratio of mean stress over von Mises equivalent stress,

$$\eta = \frac{-p}{q},$$

or principal in-plane deviatoric stress ratio,

$$\alpha = \frac{s_{min}}{s_{maj}},$$

whatever most convenient. An example of this representation is shown in Fig 2 together with a linear strain path to failure represented by the vertical arrow and nonlinear strain paths represented by the curved arrows. The dashed lines indicate the linear strain paths corresponding to uniaxial compression, shear, uniaxial tension and biaxial tension, and Table 1 lists common stress states and associated triaxiality and deviatoric stress ratio values.

_____

Table 1 Triaxiality and deviatoric stress ratio for some common stress states.

Load case	η	α
Biaxial tension	2/3	1
Plane strain tension	$1/\sqrt{3}$	0
Uniaxial tension	1/3	-1/2
Shear	0	-1
Uniaxial compression	-1/3	-2
Plane strain compression	$-1/\sqrt{3}$	$-\infty$
Biaxial compression	-2/3	1

The effective plastic strain evolves with the principal components of the plastic strain rate tensor as

$$\dot{\varepsilon}^p = \frac{2}{\sqrt{3}} \sqrt{\dot{\varepsilon}_{\min}^2 + \dot{\varepsilon}_{\text{maj}}^2 + \dot{\varepsilon}_{\min} \dot{\varepsilon}_{\text{maj}}}$$

and the safe zone is for plastic strains smaller than the critical plastic strain,

$$\varepsilon^p < \varepsilon_D^p ,$$

i.e., the area under the FLC represented in Fig 2.
Obviously nonlinear strain paths is a concern, and one way to account for this is to introduce an instability indicator

$$\omega_D \geq 0$$

that somehow evolves with plastic strain and depends on the stress state, i.e.,

$$\dot{\omega}_D = \dot{\omega}_D(\dot{\varepsilon}^p, \eta) = \dot{\omega}_D(\dot{\varepsilon}^p, \alpha) \geq 0 ,$$

and instability is said to occur when

$$\omega_D = 1 .$$

This instability model has to be accompanied with the restriction that it reconciles with the FLC representation for linear strain paths, which mathematically can be expressed as

$$\int_0^{\varepsilon_D^p} \frac{\dot{\omega}_D}{\dot{\varepsilon}^p} d\varepsilon^p = 1 \quad \text{for constant } \eta \text{ or } \alpha.$$

This suggests the following obvious evolution law,

$$\dot{\omega}_D = \frac{\dot{\varepsilon}^p}{\varepsilon_D^p} , \tag{1}$$

although there is freedom to choose any other within reason.

2.2   Post-instability and damage modelling

Independent of the model of choice to predict instability, there is the delicate matter of what happens after instability has occurred, i.e., the post-instability stage. To this end it is important to note that the reason for having an instability model in the first place is that the actual material instability phenomenon cannot be captured in the finite element model itself due to coarseness of the numerical discretization. This means that numerical results are in effect only reliable up to the instability point, and to model what really happens after that and up to the point of fracture borders to the art of

guesswork. The simplest way out would be to reconcile a fracture model with the assumption that fracture in practice occurs very soon after instability onset and whence simply erode the material when instability has been detected. If this approach leads to results that are inconsistent with the real-life behaviour then one may need to actually model the post-instability stage. A damage model can be seen as a homogenization model of the micromechanical composition of material and void that accordingly augments the stress from the constitutive model for the formation of internal forces. A simple phenomenological approach is taken by introducing a damage parameter,

$$0 \leq D < 1,$$

that is assumed to reduce the effective cross-sectional area in the direction of loading. This is to say that the homogenized stress, i.e., the stress used to model the global response, can be expressed in terms of the stress used in the constitutive law as

$$\boldsymbol{\sigma} = (1 - D)\tilde{\boldsymbol{\sigma}}, \tag{2}$$

i.e., the material is isotropically degraded with damage. This is the Continuum Damage Mechanics concept and was introduced by Lemaitre [6]. The physical interpretation of this model is usually that the area is reduced due to the formation of cavities that develop in the material during plastic loading, i.e., the material is damaged in the true sense of the word, but other interpretations may apply in the event that it just serves as a means to model, or induce, the post-instability response of the material. As the instability parameter, the damage parameter is assumed to evolve with plastic strain and depend on the stress state, but in this case we introduce two further dependencies for the following reasons.
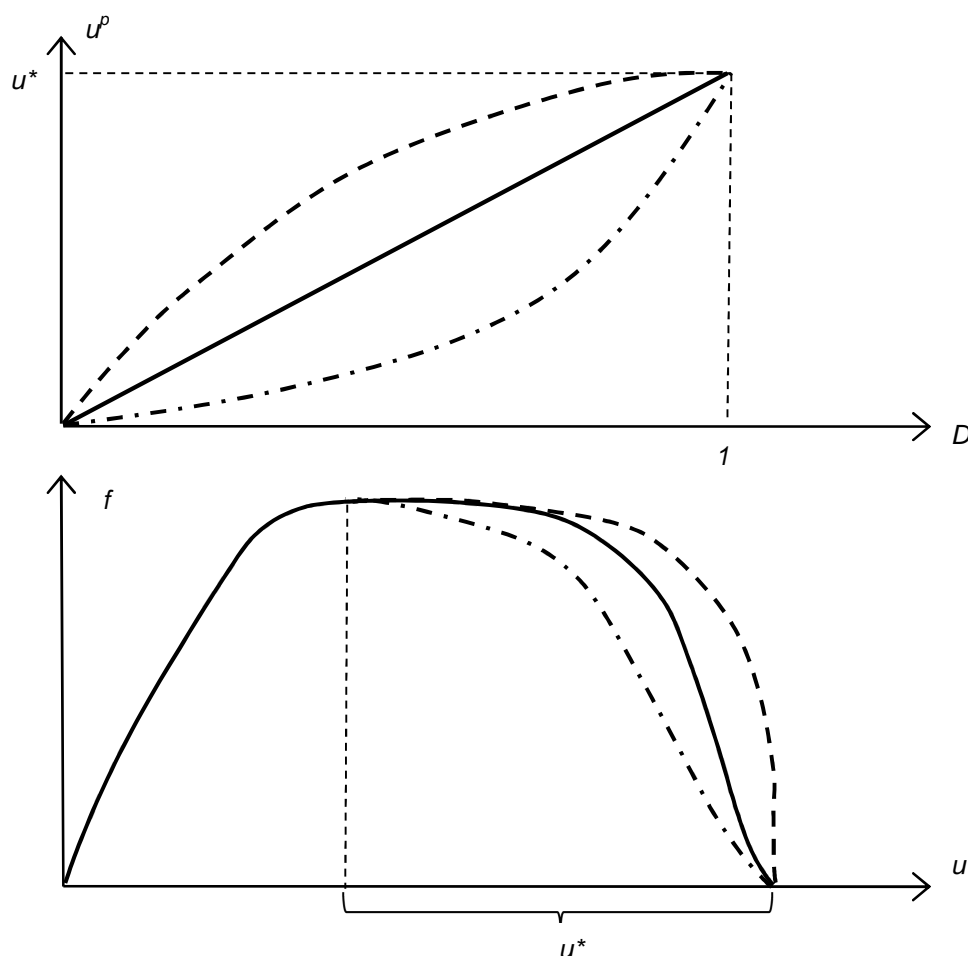
Fig 3 Hypothetical plastic displacement to failure function and the effect in a uniaxial force-displacement response.

An important aspect is that the resulting strain softening behavior that is induced by a damage model leads to results that depend highly on the numerical discretization, the finite element mesh imposes the size of the obtained localization areas and a coarse mesh is generally less prone to strain localization when compared to a fine mesh. To attenuate this effect a regularization is imperative and this is here done by that the damage parameter is assumed to depend on the mesh size h. Furthermore, in order to accurately model the shape of different engineering stress-strain responses as shown in Fig 3, a dependency on the damage parameter itself is introduced, resulting in a damage evolution law on the form

$$\dot{D} = \dot{D}(\dot{\varepsilon}^p, \eta, D, h).$$

This is further simplified by assuming that the damage evolves with the plastic displacement defined by

$$\dot{u}^p = h\dot{\varepsilon}^p \tag{3}$$

and introduce the plastic strain at failure function

$$u_f^p = u_f^p(\eta, D) \tag{4}$$

and the resulting damage evolution as

$$\dot{D} = \frac{\dot{u}^p}{\dfrac{\partial u_f^p}{\partial D}(\eta, D)}. \tag{5}$$

The interpretation of the plastic strain at failure function is illustrated in a uniaxial tension case ($\eta=1/3$) in Fig 3, where the value at $D=1$ governs the elongation of a test specimen between instability and fracture while the appearance governs the tail shape of the force displacement curve.

3   The DIEM model

The DIEM model is thoroughly treated in the LS-DYNA keyword manual on *MAT_ADD_EROSION [7], and should be read in parallel to the following.

3.1   Combining criteria

The DIEM model allows for an arbitrary number of initiation and evolution criteria to be defined and combined. Assuming that n initiation/evolution types have been defined, damage initiation and evolution history variables $\omega_D^i \in [0, \infty[$ and $D^i \in [0,1]$, $i=1,...n$, are introduced for each integration point. These are initially set to zero and then evolve with the deformation of the elements according to rules associated with the specific damage initiation and evolution type chosen. The damage initiation variables do not influence the results but just serve as an indicator for the onset of damage. The damage evolution variables govern the damage in the material and are used to form the global damage $D \in [0,1]$. When multiple criteria are active, $n>1$, each individual criterion can be of maximum, $i \in I_{\max}$, or multiplicative, $i \in I_{\mathrm{mult}}$, type. The global damage variable is defined as

$$D = \max(D_{\max}, D_{\mathrm{mult}})$$

where

$$D_{\max} = \max_{i \in I_{\max}} D^i$$

$$D_{\mathrm{mult}} = 1 - \prod_{i \in I_{\mathrm{mult}}} (1 - D^i)$$

Now to the evolution of the individual damage initiation and evolution history variables, and for the sake of clarity we skip the superscript *i* from now on.

3.2 Initiation criteria

3.2.1 Ductile criterion

For the ductile initiation option a function $\varepsilon_D^p = \varepsilon_D^p(\eta, \dot{\varepsilon}^p)$ represents the plastic strain at onset of damage. Optionally this function can depend on the effective plastic strain rate $\dot{\varepsilon}^p$. The damage initiation history variable evolves according to

$$\omega_D = \int\limits_0^{\varepsilon^p} \frac{d\varepsilon^p}{\varepsilon_D^p}.$$

3.2.2 Shear criterion

For the shear initiation option a function $\varepsilon_D^p = \varepsilon_D^p(\theta, \dot{\varepsilon}^p)$ represents the plastic strain at onset of damage. This is a function of a shear stress function defined as

$$\theta = (q + k_S p)/\tau$$

with *p* being the pressure, *q* the von Mises equivalent stress and τ the maximum shear stress defined as a function of the principal stress values

$$\tau = \left(\sigma_{\mathrm{major}} - \sigma_{\mathrm{minor}}\right)/2.$$

Introduced here is also the pressure influence parameter k_s. Optionally this function can depend on the effective plastic strain rate $\dot{\varepsilon}^p$. The damage initiation history variable evolves according to

$$\omega_D = \int\limits_0^{\varepsilon^p} \frac{d\varepsilon^p}{\varepsilon_D^p}.$$

3.2.3 MSFLD and FLD criteria

The MSFLD and FLD initiation options are restricted to plane stress shell elements, and only the mid-surface is considered in an attempt to characterize the cross section as a whole. For this a function $\varepsilon_D^p = \varepsilon_D^p(\alpha, \dot{\varepsilon}^p)$ represents the plastic strain at the onset of damage. Optionally this can function can also depend on the effective plastic strain rate $\dot{\varepsilon}^p$, which must be positive for the initiation variable to evolve.

For the MSFLD criterion, the plastic strain used in this failure criterion is a modified effective plastic strain that only evolves when the pressure is negative, i.e., the material is not affected in compression. The damage initiation history variable evolves according to

$$\omega_D = \max_{t \leq T} \frac{\varepsilon^p}{\varepsilon_D^p},$$

which should be interpreted as the maximum value up to this point in time. In effect, this means that damage starts evolving as soon as the (modified) plastic strain reaches the critical value. The FLD option differs from the MSFLD option in that the damage initiation history variable evolves just as the ductile and shear criteria, i.e.,

$$\omega_D = \int\limits_0^{\varepsilon^p} \frac{d\varepsilon^p}{\varepsilon_D^p}.$$

and by that the plastic strain here is *not* modified by the sign of pressure.
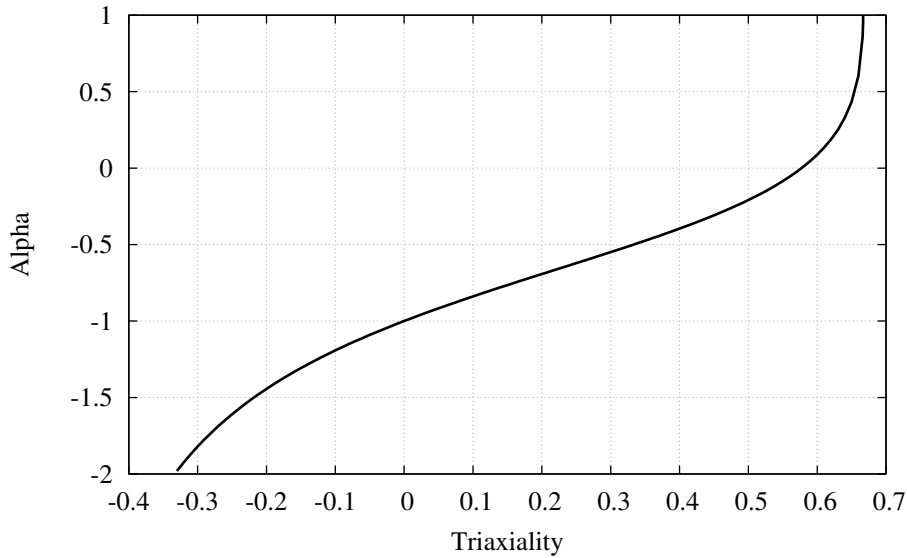
Fig 4 MSFLD input principal stress ratio vs. triaxiality.

The MSFLD (and FLD) instability curve is with respect to the ratio of principal deviatoric stress components in the plane, α, and as a reference we present here the conversion formulae between this quantity and the triaxiality η. This relation is obtained via the following two relations, assuming $\eta>-1/3$, and parametrized in $\beta>-1$

$$\alpha = -\frac{2\beta+1}{2+\beta}$$

$$\eta = \frac{1-\beta}{3\sqrt{1+\beta+\beta^2}}$$

and is shown in Fig 4. Table 1 lists some of these relations.

3.3 Evolution criteria

For the evolution of the associated damage variable *D* we introduce the plastic displacement u^P which evolves according to

$$\dot{u}^p = \begin{cases} 0 & \omega_D < 1 \\ h\dot{\varepsilon}^p & \omega_D \geq 1 \end{cases}$$

with *h* being a characteristic length of the element introduced to suppress the mesh dependence often encountered in finite element damage models. Note that this quantity starts evolving after the corresponding damage initiation variable reaches unity and also that each criterion has its unique plastic displacement variable.

3.3.1 Linear damage evolution

The damage variable evolves linearly with the plastic displacement according to

$$\dot{D} = \frac{\dot{u}^p}{\frac{\partial u_f^p}{\partial D}}$$

with u_f^p being the plastic displacement at failure function. The plastic displacement at failure can be constant or depend on the triaxiality and damage, which in the latter case means that $u_f^p = u_f^p(\eta, D)$. This can be used to characterize and differentiate the post-instability stage by designing this function according to the illustration in Fig 3.

_____

4   Examples
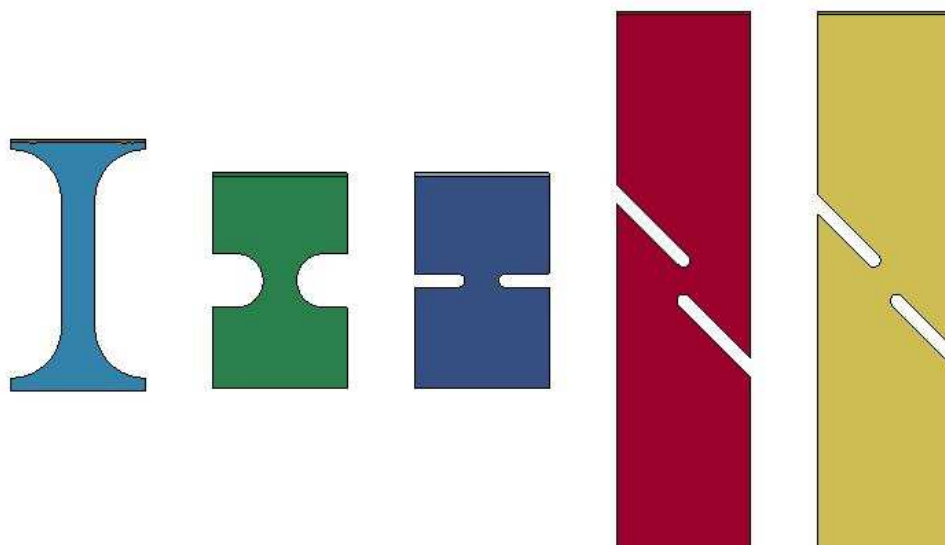
Fig 5 Specimens for calibrating the DIEM model (A10,R4,R1,S0 and S30).

4.1   Crude calibration of the DIEM model

Fig 5 shows some specimens (labeled as in the caption) developed at Fraunhofer IWM, Freiburg, Germany, under the supervision of Dr. Dong-Zhi Sun. When elongated in the vertical direction these are subjected to a reasonably homogenous stress state in the deformation region with triaxiality values as listed in Table 2. The purpose of this example is to design damage initiation and evolution parameters to get the failure characteristics of the aluminium alloy EN-AW 6082 in temper T6 supplied by SAPA. We use the FLD initiation criterion in Section 3.2.3 and want to find the critical plastic strains for the triaxiality values in Table 2, and thereafter use a damage evolution law as in Section 3.3.1 to find the table giving critical plastic displacement as function of triaxiality and damage. Although damage and plastic deformation are two distinct dissipative processes they influence each other, and furthermore the stress state is not homogeneous in the specimens, which makes the calibration of the model non-trivial and an optimization tool such as LS-OPT is generally recommended. The estimation of the DIEM parameters was done manually and intuitively, with results reflecting this fact.

Table 2 Rough triaxiality value for the different specimens shown in Fig 5.

Specimen	Triaxiality
A10	0.33
R4	0.45
R1	0.66
S0	0.0
S30	0.2

In Fig 6, the results from the parameter calibrations for GISSMO and DIEM are shown, of which the former is done with LS-OPT. One immediate conclusion can be drawn, being that a perfect fit to tests for all the specimens is simply out of reach. This can be at least partly attributed to the complex mechanisms occurring in the post-instability region of the different tests, i.e., the coupling and transition between different stress states. A more complex model and better understanding of micromechanical effects are probably needed to obtain a better fit. It can also be seen that the optimization of the GISSMO model leads to a result seemingly different from (and perhaps better than) the DIEM results, which is probably explained by the difference in approach as the latter is obtained through manual tweeking of parameters with lack of systemacy.

A10

R1

R4

S0

S30
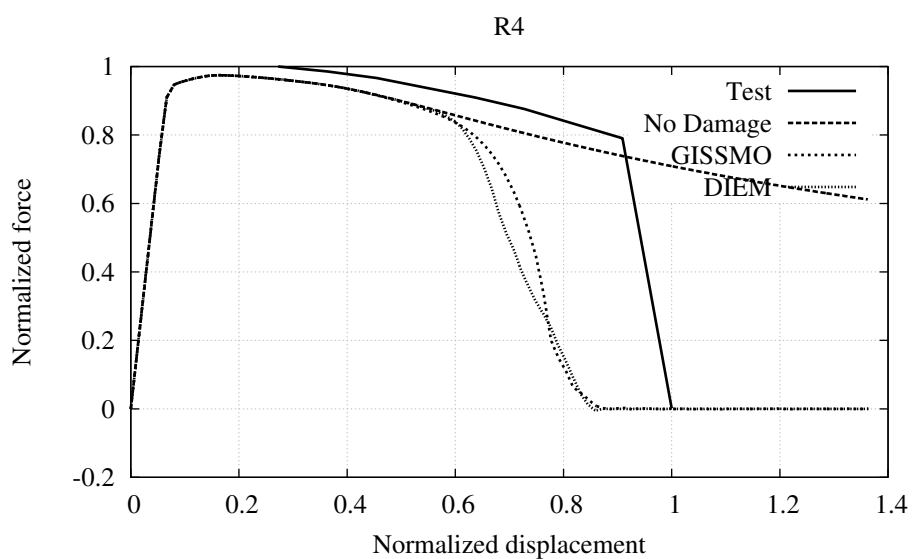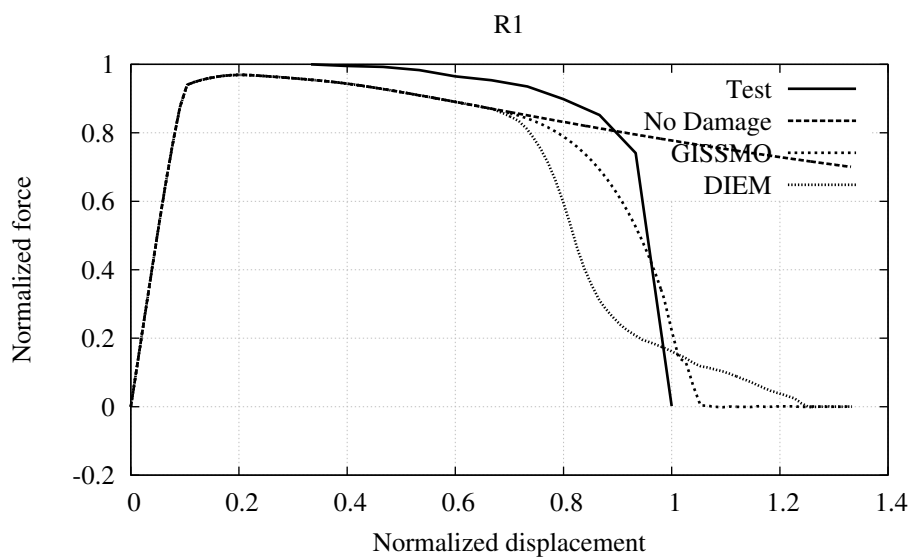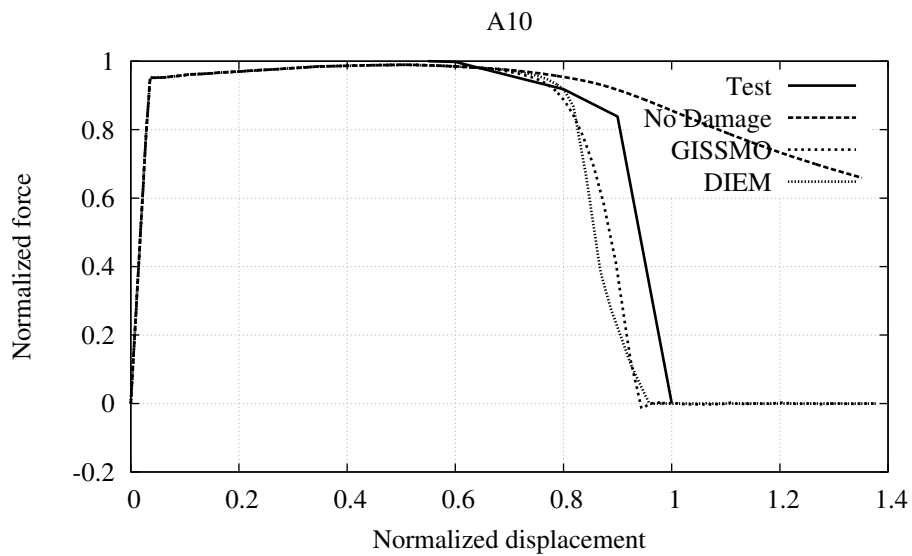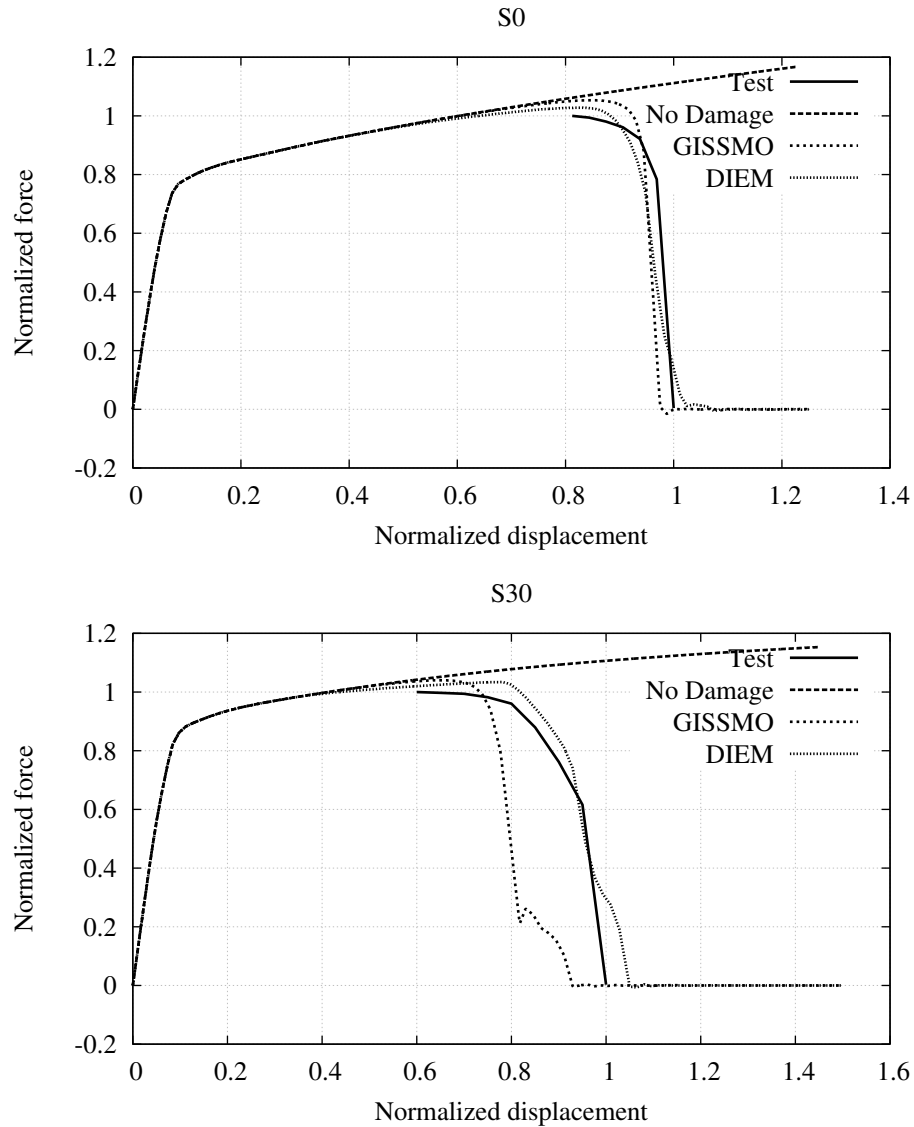
Fig 6 Results from model calibration for GISSMO and DIEM.

It is here appropriate to discuss the results from a comparative perspective and briefly summarize the differences between GISSMO and DIEM. The GISSMO damage evolution model is of the form (5), but where the plastic displacement and plastic displacement at failure are defined by

$$\dot{u}^p = r(h)\dot{\varepsilon}^p$$

and

$$u_f^p = r(h_{\text{ref}})\varepsilon_f^p(\eta)D^\gamma\varphi(\dot{\varepsilon}^p)\,, \qquad (6)$$

respectively. The introduction of a regularization function r and a strain rate scaling function φ makes the model more general, while the actual damage evolution law is a γ-parameterized restriction of the more general expression (4). Furthermore, the Lemaitre-type coupling to the stress as in (2) is generalized in GISSMO by introducing an exponent δ,

$$\boldsymbol{\sigma} = (1 - D^\delta)\tilde{\boldsymbol{\sigma}}\,,$$

which together with the exponent γ can be used to determine the post-instability behaviour of the material. The damage initiation model in GISSMO is analogous to that of its evolution model defined

by (6) except for no element size dependency. The initiation model utilizes the same exponent γ and strain rate scaling function φ as in the evolution model. This should be compared to the DIEM correspondence in (1), which is a simplified variant of the GISSMO counterpart except for a more general strain rate dependence. For linear strain paths they more or less amount to the same thing, but GISSMO allows for more flexibility when it comes to fitting the instability onset for nonlinear strain paths. All in all the two models are similar and regardless of preference, the performance hinges mostly upon how well the damage initation and evolution parameters are fit to reflect the failure characteristics of the material of interest.

4.2 DIEM and CrachFEM

Some single element examples with different strain paths will be used to illustrate the DIEM model and compare it to two alternative failure prediction models: CrachFEM by Matfem [4] and the standard LS-Dyna model MAT190 [7], an anisotropic elastic-plastic material model with a strain based failure criterion. The material used is a relatively brittle high strength steel. Hence failure can be assumed to occur close to instability and therefore only damage initiation is considered. The FLD criterion is used and although the Ductile and Shear criteria are also included in the model, they are never critical.

4.2.1 Linear strain path

In Fig 7, constant uniaxial tension is applied until failure. We can see that all three models behave as expected with failure at the FLC, both in the $\varepsilon_D^p = \varepsilon_D^p(\eta)$ and the $\varepsilon_{maj}^* = \varepsilon_{maj}^*(\varepsilon_{min})$ diagrams.
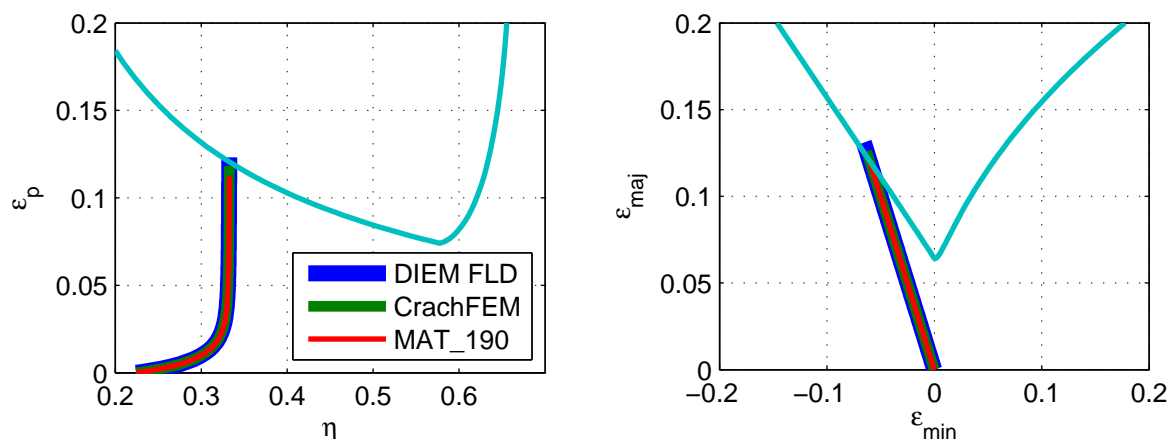
Fig 7 Linear strain path example, uniaxial tension.

4.2.2 Non-linear strain paths

When first applying uniaxial tension and then switching to plane-strain loading, see Fig 8, we see that the behaviour looks different in the two different variable spaces. We must then remember that in DIEM, the FLD is given as $\varepsilon_D^p = \varepsilon_D^p(\eta)$ and in MAT190 it is given as $\varepsilon_{maj}^* = \varepsilon_{maj}^*(\varepsilon_{min})$. The translation between the two is only straight forward as long as the strain path is linear. The situation is similar in Fig 9, where the load is first biaxial tension and then plane-strain.

In DIEM, the damage initiation (and evolution, not considered here) variables are stored as extra history variables in D3PLOT and ELOUT. More or less corresponding variables are available in CrachFEM and MAT190. A comparison for the last example is shown in Fig 10. The staggered look of the CrachFEM FLD curve is due to fact that the rather costly Crach algorithm is only evaluated with a certain plastic strain interval, in this case 2%.
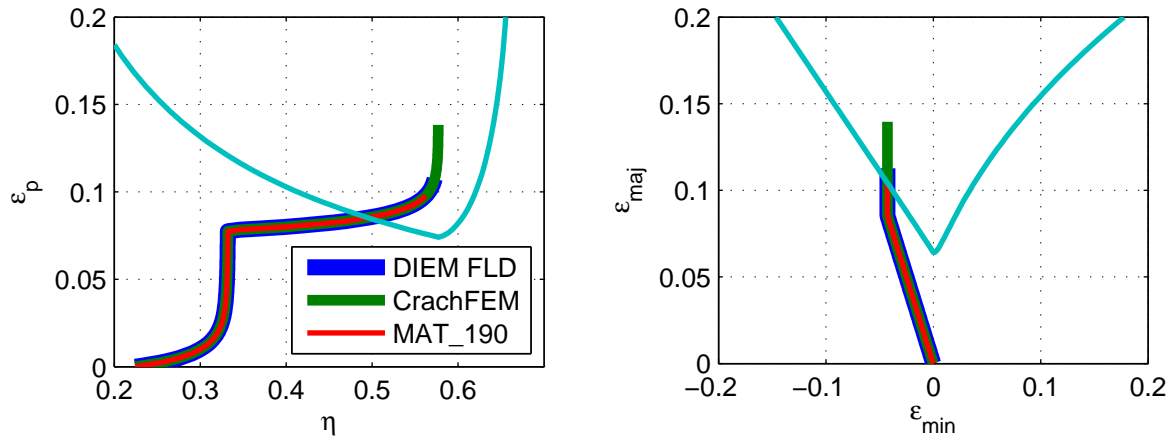
Fig 8 Non-linear strain path example, uniaxial tension + plane strain.
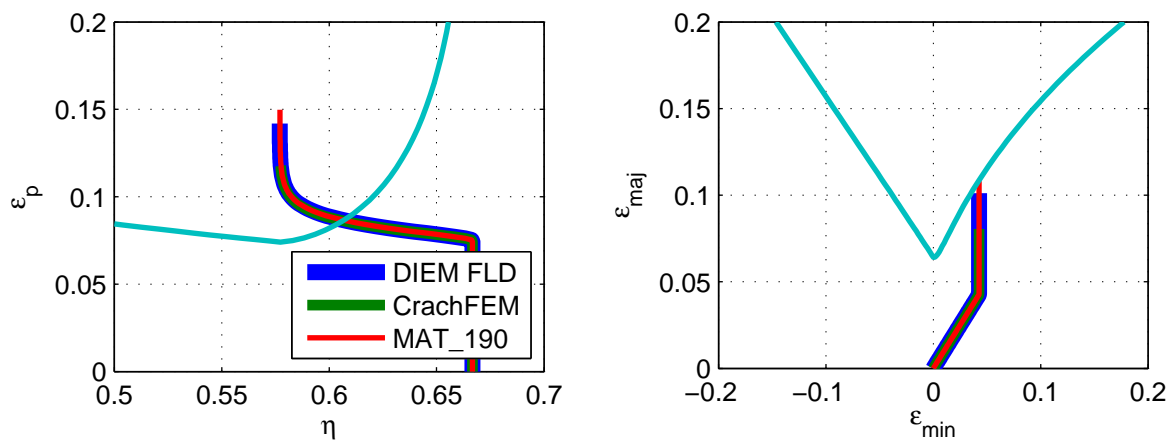
Fig 9 Non-linear strain path example, biaxial tension + plane strain.
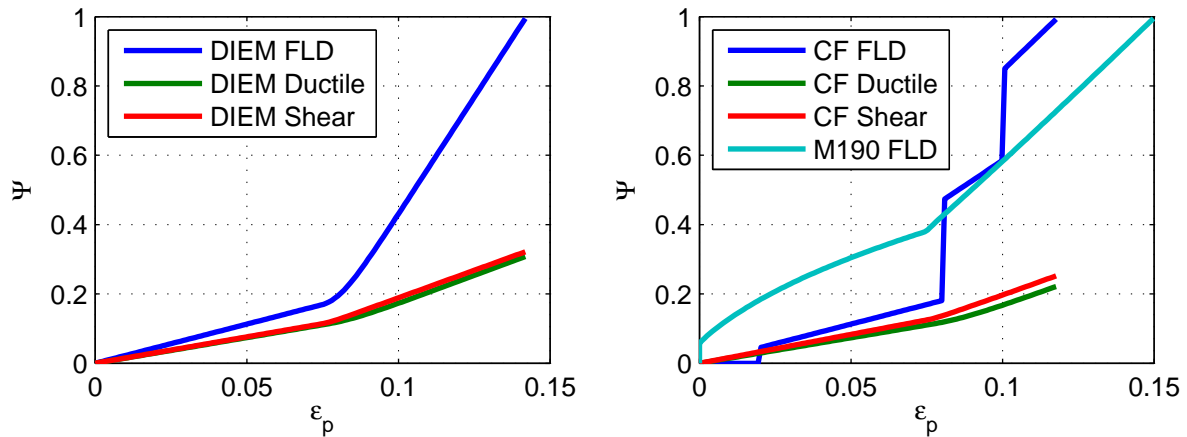
Fig 10 Damage initiation (or failure risk) variables in non-linear strain path example (CF = CrachFEM).

4.3   Comparison between MSFLD and FLD in DIEM

As described in Section 3.2.3 above, two different instability criteria are available in DIEM. In order to illustrate the difference between them, we will study an example where we start near pure shear loading and then go to uniaxial tension. However, as we start either slightly into the compressive or the tensile region, we will see completely different behaviour of DIEM MSFLD in Fig 11. This is due to the effect of pressure sign in the MSFLD criterion that is not present in the FLD criterion.
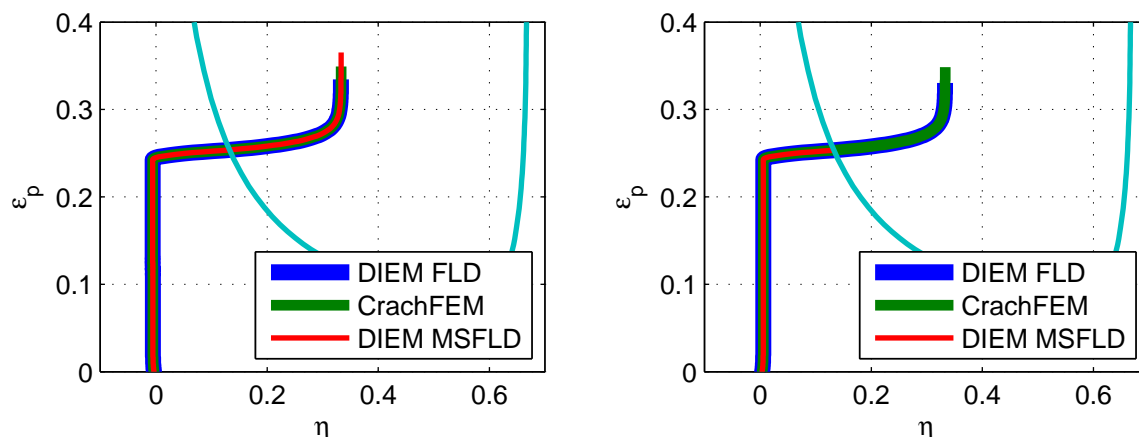
Fig 11 LHS – starting with $\alpha = -1.01$, RHS – starting with $\alpha = -0.99$.

5   Summary

The keyword MAT_ADD_EROSION in LS-DYNA is today equipped with two damage initiation and evolution models, GISSMO and DIEM, and this paper has been exploiting the features of the latter. A comparison can conclude that the two models are very similar in terms of functionality with a few exceptions. One fundamental difference is that the DIEM model can be used to predict instabilities in forming applications with shell elements using an FLD criterion that attempts to consider the characteristics of the cross section and not each integration point individually. Except for this, the differences lie mostly in the mathematical expressions of the instability and evolution criteria, and either model could be preferable as it comes down to how well test data can be fitted within the realm of parametrization. One aspect in terms of preferring one over the other is the matter of taste and comfort, and from this aspect the users of CrachFEM could find DIEM attractive as it is apparently similar in that several criteria can be combined. With a positive mindset, DIEM can be seen as CrachFEM light. Two examples have been presented to highlight these conclusions.

6   Acknowledgments

The authors are grateful to SAPA Technology and Fraunhofer IWM for allowing data to be used for completing this document.

7   References

[1]   Neukamm F., Feucht M. and Haufe A., Considering Damage History in Crashworthiness
        Simulations, Proc. 7th Eur. LS-DYNA Users Conf., Salzburg, Austria, 2009.
[2]   Haufe A., Neukamm F., Feucht M. and Borrvall T., A Comparison of Recent Damage and
        Failure Models for Steel Materials in Crashworthiness Application in LS-DYNA, Proc. 11th Int.
        LS-DYNA Users Conf., Dearborn, MI, USA, 2010.
[3]   Effelsberg J., Haufe A., Feucht M., Neukamm F. and DuBois P., On Parameter Identification for
        the GISSMO Damage Model, Proc. 12th Int. LS-DYNA Users Conf., Dearborn, MI, USA, 2012.
[4]   CrachFEM, *www.matfem.de*
[5]   Marciniak Z. and Kuckzynski K., Limit Strains in the Process of Stretch-Forming Sheet Metal,
        Int. J. Mech. Sci., 9, pp. 609-620, 1967.
[6]   Lemaitre J., A Continuous Damage Mechanics Model for Ductile Fracture, J. Mat. Tech., 107,
        pp. 83-89, 1985.
[7]   LS-DYNA Keyword User's Manual, R7.0.0, Volume II Material Models, Livermore Software
        Technology Corporation (LSTC), 2012.